Iranian Journal of Chemistry and Chemical Engineering (IJCCE)

www.ijcce.ac.ir

Expired Actifed Drug as Corrosion Inhibitor for Low-Carbon Steel in Phosphoric Acid: Experimental and Theoretical Investigation

Rana A. Anaee

Department of Materials Engineering, University of Technology, Baghdad, Iraq

Nanotechnology and Advanced Materials Research Center, University of Technology, Baghdad, Iraq

Haydar A. S. Aljaafari*

Department of Chemical Engineering, University of Technology, Baghdad, Iraq

Shaimaa A. Naser

Nanotechnology and Advanced Materials Research Center, University of Technology, Baghdad, Iraq

Anees A. Khadom

Department of Chemical Engineering, University of Diyala, Baqubah, Iraq.

Ali M. Abd

Nanotechnology and Advanced Materials Research Center, University of Technology, Baghdad, Iraq

Tamara A. Anai

Tikrit University, Dentistry Basic Science, Tikrit, Iraq.

Abstract

Corrosion remains a significant challenge for industrial infrastructure and equipment made from low-carbon steel, especially in acidic environments. Inhibitors have proven effective in mitigating corrosion, and expired pharmaceuticals offer an innovative class of potential solutions. This study explores the use of expired Actifed (ACD) as a sustained corrosion inhibitor for low-carbon steel in a 0.5 M H_3PO_4 solution. Both experimental and theoretical approaches were employed to assess the inhibitor's efficiency. Experimental techniques included potentiodynamic polarization (PDP), Scanning Electron Microscopy (SEM), Fourier Transform Infrared Spectroscopy (FTIR), and microbiological tests. Theoretical evaluations utilized quantum chemical calculations to investigate how ACD interacts with the steel surface. The findings indicated that ACD significantly decreases the corrosion rate, resulting in an inhibition efficiency of 73.5% under the conditions (concentration of 60 mL/L and a temperature of 303 K). It was observed that ACD forms protective layers on the steel, providing mixed protection for both anodic and cathodic sites. The outcomes from FTIR, SEM, and theoretical studies corroborate the electrochemical findings, confirming the effectiveness of Actifed as an inhibitor under the selected conditions.

Keywords: Actifed expired drug; low-carbon steel; phosphoric acid; polarization; corrosion; inhibitor; DFT.

1. Introduction

Steel alloys are commonly used in numerous industries due to their excellent machining ability, high plasticity and toughness, and inexpensive cost [1]. The chemical industry's rapid growth has led to a worsening service environment for equipment components, resulting in economic losses due to corrosion. Additionally, operational safety issues are becoming more prevalent, particularly in acidification construction processes, which can lead to severe corrosion [2]. As a result, corrosion prevention remains a critical concern [3]. Metal corrosion can be prevented by organic coatings [4], cathodic protection [5], anode protection [6], and corrosion inhibitors [7]. Adding corrosion inhibitors can cause physical and chemical reactions on the metal surface, creating a protective coating. Corrosion inhibitors are typically organic molecules with heteroatoms or heterocycles and unsaturated linkages with different sources of electron density [8] that work by adsorption process, but the higher temperatures often decrease this adsorption by enhancing reaction kinetics, which can weaken the adsorbed inhibitor film and increases the movement of ions and electrons. These organic molecules have many advantages in their molecular formula assist in adsorption process such as 2-mercaptobenzothiazole (MBT) and 2-amino benzothiazole (ABT) compounds [9], novel N_2O_4 Schiff-base Ligands [10], N, N′-bis(4-formyl phenol)-trimethylene diamine Schiff base [11], a novel green material [12], N, N′-Bis(phloroacetophenone)-1,2-propane diamine [13], synthetic symmetrical Schiff bases [14], Thiobarbituric acid and Thiourea compounds [15], and new reduced Schiff base ligand [16].

Inorganic inhibitors are limited by their toxicity, which poses risks of environmental pollution and negative health effects. Conversely, organic inhibitors are categorized into natural and synthetic types. Synthetic organic inhibitors are produced through artificial synthesis, leading to an intricate and expensive manufacturing process [17]. As a result, research is urgently needed to find an efficient and eco-friendly alternative inhibitor. Plant extracts and expired drugs represent alternative sources. Plant extracts must be collected, cleaned, dried, extracted, filtered, and concentrated before use. This is a time-consuming process [18].

The use of medicines as corrosion inhibitors has recently increased. These pharmaceuticals outperform typical inhibitors in terms of environmental friendliness. Drugs have replaced traditional, harmful corrosion inhibitors since they are safer and have fewer adverse ecological consequences. A drug is used as a corrosion inhibitor because it contains donor atoms such as O, N, and S. Furthermore, drugs are environmentally friendly, have biological applications, and are simple to prepare and purify. During the last decades, many authors highlighted the addition of expired medications as green inhibitors for steel alloys in different environments, such as fluoroquinolones [19], tarivid [20], ranitidine [21], cefixime [22], antihypertensive drugs [23], antibiotic derivatives [24], amoxicillin [25], amodiaquine [26], farcolin [27], atorvastatin [28], sulpha drugs [29], levofloxacin [30], etoricoxib [31], metoclopramide [32], isosorbide dinitrate [33], spiramycin [34, 35], metheprim [36], butamirate [37]. These drugs have demonstrated effective inhibition properties in various settings, including their role when surgically implanted inside the body [38, 39]. In addition to pharmaceuticals, other green materials, such as Salicornia extract [40], Bhumyamalakhi [41], Trachyspermum leaves [42], Lavendula stoechas extract [43], active oleic imidazoline, 2-mercaptobenzimidazole [44], Mentha spicata extract [45], and matured cocoa pod extract [46], have also been confirmed as effective inhibitors.

Despite the promising results with other drugs, limited research has investigated the potential of Actifed as a corrosion inhibitor. This study aims to address this gap by evaluating the efficacy of expired Actifed Drug (ACD) in inhibiting the corrosion of carbon steel in (0.5 M) H_3PO_4 solution. Electrochemical techniques were used to conduct the experiments. SEM and FTIR techniques were used for surface morphological and diagnosis studies. Kinetics and adsorption studies were utilized to assess the drug's performance. Quantum chemical theoretical studies supported the experimental outcomes.

2. Experimental Procedure

2.1 Specimens and electrolyte

A carbon steel plate with a weight percentage of 0.0979 C, 0.185 Si, 0.551 Mn, 0.0069 P, <0.0005 S, 0.0077 Cr, 0.0193 Ni, 0.0072 Cu, 0.0332 Al, and the balance is Fe was cut into specimens with dimensions of 10mm×10mm×4mm. These specimens were subjected to grinding and polishing to get a mirror surface and kept for electrochemical testing [47]. The corrosive electrolyte 0.5 M H_3PO_4 was prepared by diluting concentrated 85% H_3PO_4. Expired (ACD) syrup contains 6 mg/ml of *pseudoephedrine hydrochloride*, and 0.25 mg/ml *triprolidine hydrochloride* was used as a corrosion inhibitor. The inhibitor's effectiveness was evaluated at the following concentrations: 4, 20, 40, and 60 mL of ACD per liter of 0.5 M H_3PO_4 [31].

2.2 Characterization

Various techniques were utilized to characterize the inhibited surface, including FTIR from Bruker and SEM from TESCAN, Czech Republic. The antibacterial properties of ACD were tested using the Well *Diffusion Method*, which comprised the preparation of Mueller-Hinton (MH) Agar and a diffusion well assay. This test aims to evaluate whether ACD can help reduce microbiological corrosion. Since ACD is a pharmaceutical product, it's essential to check if it can also limit bacterial growth, which may offer additional protection to the metal surface in environments where both corrosion and microbial activity could be an issue.

The microbiological test was conducted as follows: Mueller-Hinton (MH) agar was prepared by adding 38 grams of dried Mueller-Hinton agar powder into 1L of distilled water, mixed, and then heated to fully dissolve the agar powder. The agar was autoclaved for fifteen minutes at 121°C. Then, it was distributed into sterile Petri dishes to a depth of 4 mm. A bacterial suspension of *Staphylococcus aureus* and *E. coli* was prepared with the standard of 0.5 McFarland turbidity (≈ 1.5×10^8 CFU/mL) for the diffusion well test. The bacterial solution was dispersed uniformly over the surface of the MH agar in the prepared petri dishes. After complete absorption of the bacterial solution, a sterile cork borer was used to make wells of 5 mm diameter in the agar. ACD solution was then added to each well at a volume of 0.1 mL. Finally, the dishes were placed in the incubator for 24 hours at 37 °C before the growth inhibitory zones were investigated in millimeters (mm) [32].

2.3 Corrosion measurements

Three electrode cells (working, reference, and auxiliary) were used, which were connected to a potentiostat instrument from Corrtest CS٣٥0 using CS Studio 6 software. The potential-time relationship was recorded with a Saturated Calomel Electrode (SCE). Polarization curves were then obtained by applying potentials of +200 mV around the open circuit

potential to measure the corrosion potential, corrosion current density, and the cathodic and anodic Tafel slopes. Four experimental temperatures (303, 313, 323, and 333 K) were controlled using a jacketed cell connected to a circulating bath of water. These temperatures were selected to replicate typical conditions for pipelines exposed to atmospheric temperatures during both winter and summer. The detailed electrochemical procedure is described in previous studies [48, 49].

3. Results and discussion

3.1 Electrochemical studies

The first interaction between materials and the environment can be estimated by potential-time observation to record open circuit potential (Eoc), which correlates with the potential difference of the electrical double layer as described by Helmholtz. Equilibrium is established when the electrons leave the metal lattice structure to form a layer of ions that interact to produce solvated ions with the metal electrode through electrostatic force. This behavior in the presence and absence of Actifed is illustrated in Fig. 1, which shows the shifting of the behavior of carbon steel toward a noble direction, referring to the formation of a protective layer on the metal surface due to the influence ACF. The value of (E_{oc}) for carbon steel in blank solution was recorded as -0.575 V, and in the presence of 4, 20, 40, and 60 mL/L Actifed, the values were -0.559, -0.558, -0.553, and -0.551 V, respectively.

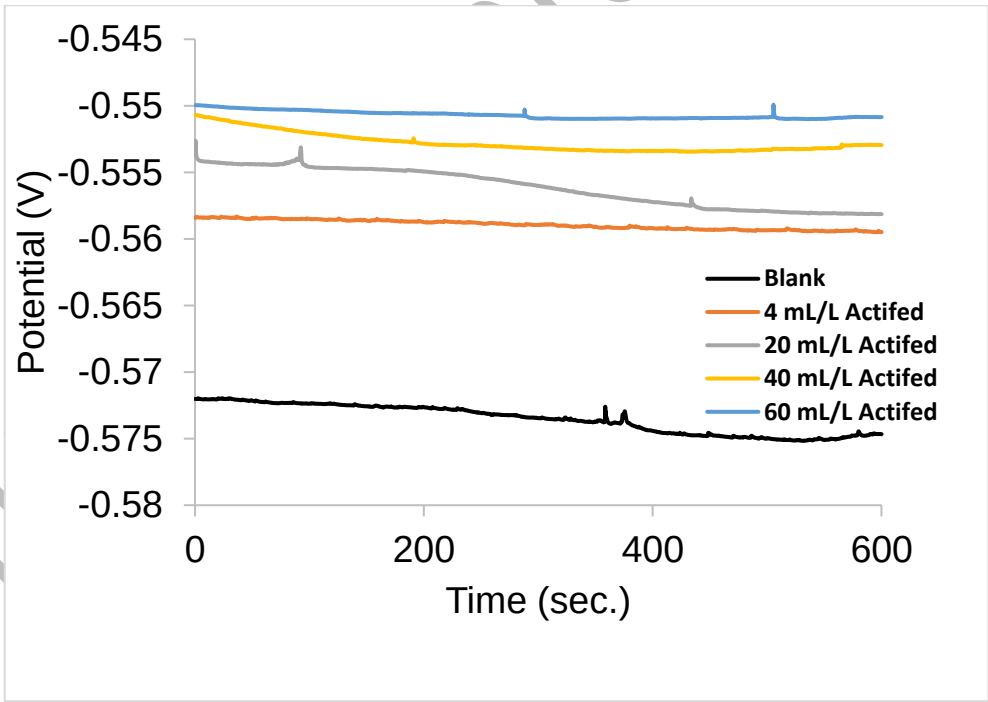

Fig. 1 Potential-time illustration for carbon steel in the presence and absence of ACD.

The corrosion behavior can be estimated by recording the Tafel plot (polarization curve), which illustrates the cathodic behavior in the lower section and the anodic behavior in the upper section, where at the cathodic sites, the reduction reaction takes place. In the acidic medium, the evolution of molecular hydrogen is represented by the following:

$$2H^+ + 2e \rightarrow H_2 \uparrow \quad (1)$$

While at anodic sites, the dissolution of metals can occur as follows:

$$Fe \rightarrow Fe^{2+} + 2e \quad (2)$$

Fig. 2 shows Tafel plots for carbon steel in the presence and absence of ACD at different temperatures. The electrochemical data for these curves is listed in Table 1. The results showed that adding the drug slightly shifted the corrosion potential (Ecorr), indicating that they act as organic inhibitors, forming a protective hydrophobic layer of adsorbed molecules on the metal surface by solubility or dispersibility in the corrosive medium. The effectiveness of an adsorbed inhibitor depends on its chemical structure (size), aromaticity, and the number and type of bonding atoms (N atom and π). In addition, it depends on the nature of the bonding strength, and the charges of the metal surface (substrate) and its ability to form a stable complex with atoms within the metal lattice. The decrease in corrosion current density values (i_{corr}) refers to providing a barrier that hinders the metal's dissolution in the electrolyte. Furthermore, the reduction in Tafel slopes (bc and ba) indicates a decrease in cathodic and anodic sites and a reduction in their reactions. Additionally, the inhibition efficiency (%IE) was calculated using Eqs. 3 [50, 51], and the results are presented in Table 1. The results reveal that inhibition efficacy increases with concentration but declines as the temperature rises. The highest efficiency (73.5%) was observed at a concentration of 60 mL/L and a temperature of 30°C.

$$IE\% = \left[1 - \frac{i_{corr\ in\ presence\ Actifed}}{i_{corr\ in\ absence\ Actifed}}\right] \times 100 \quad (3)$$

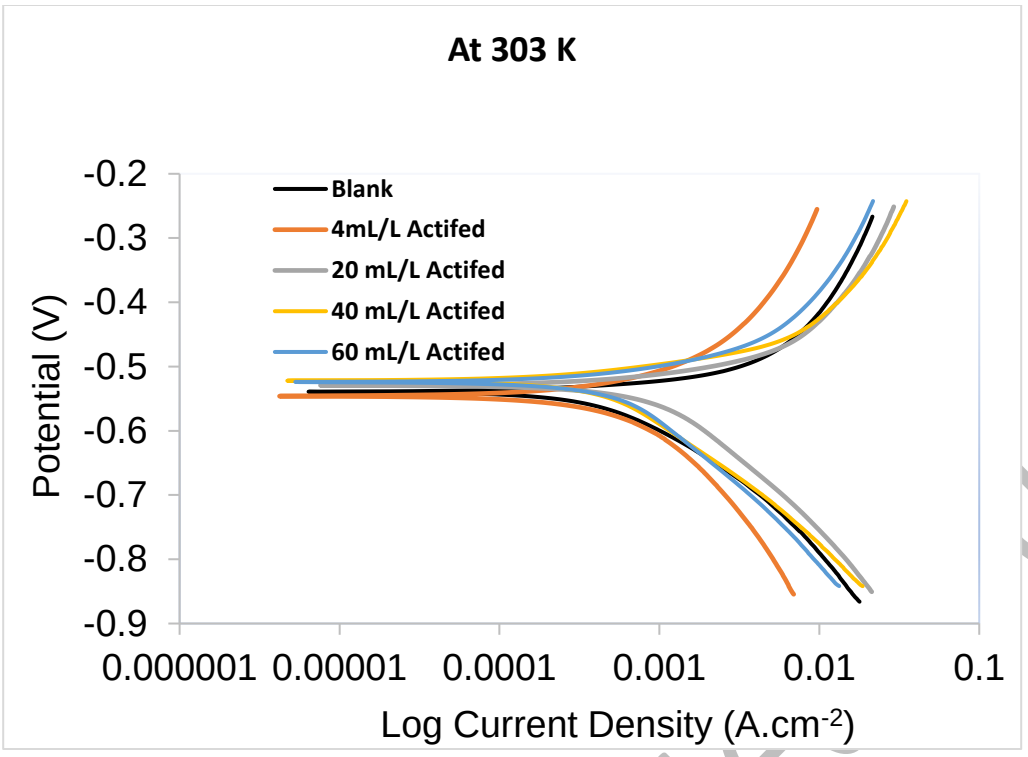
At 303 K
Blank
4mL/L Actifed
20 mL/L Actifed
40 mL/L Actifed
60 mL/L Actifed
Potential (V)
-0.2
-0.3
-0.4
-0.5
-0.6
-0.7
-0.8
-0.9
0.000001
0.00001
0.0001
0.001
0.01
0.1
Log Current Density (A.cm-2)

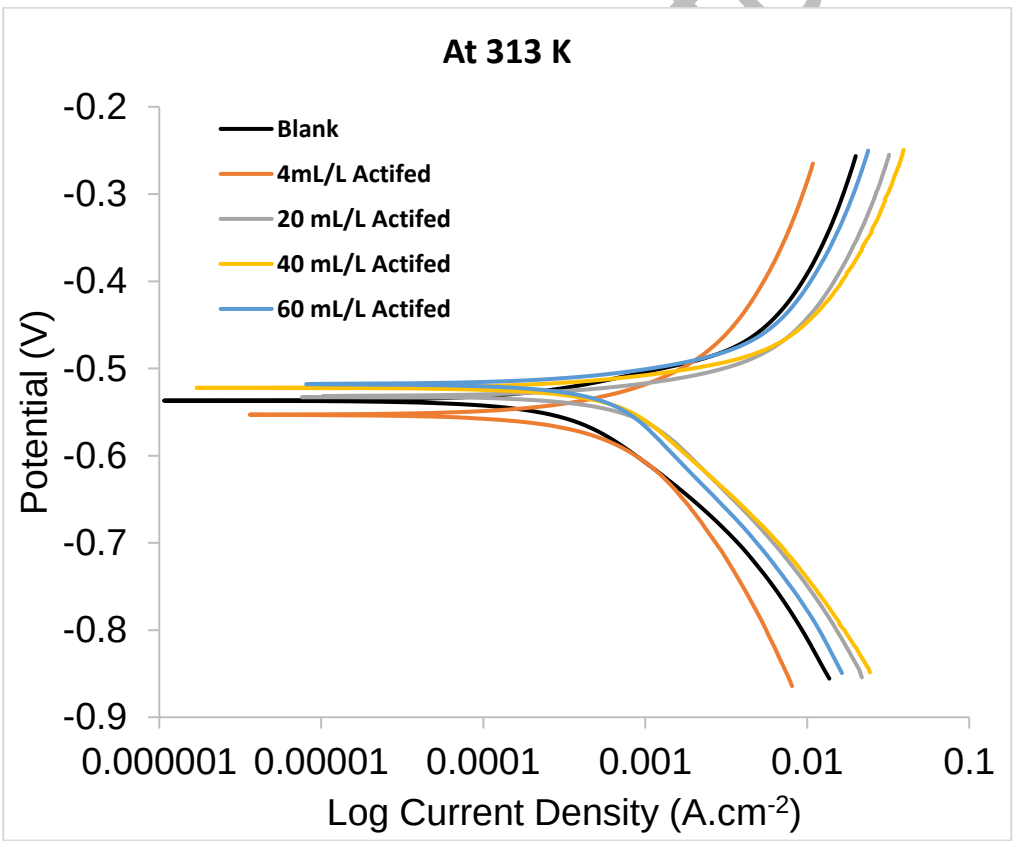
At 313 K
Blank
4mL/L Actifed
20 mL/L Actifed
40 mL/L Actifed
60 mL/L Actifed
Potential (V)
-0.2
-0.3
-0.4
-0.5
-0.6
-0.7
-0.8
-0.9
0.000001
0.00001
0.0001
0.001
0.01
0.1
Log Current Density (A.cm-2)

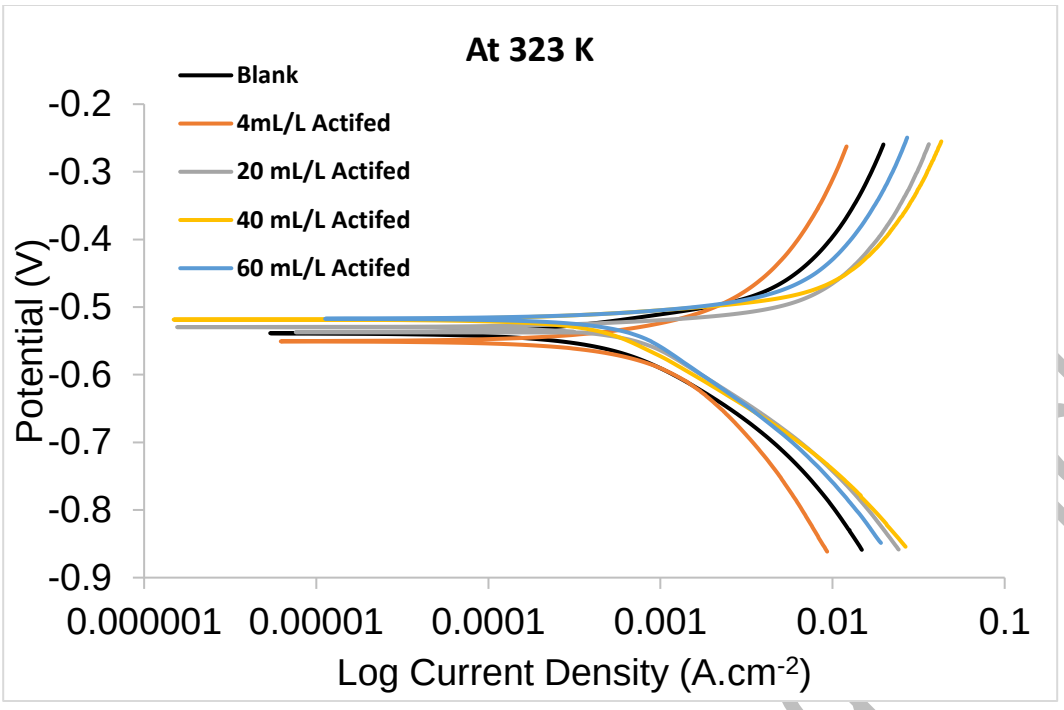

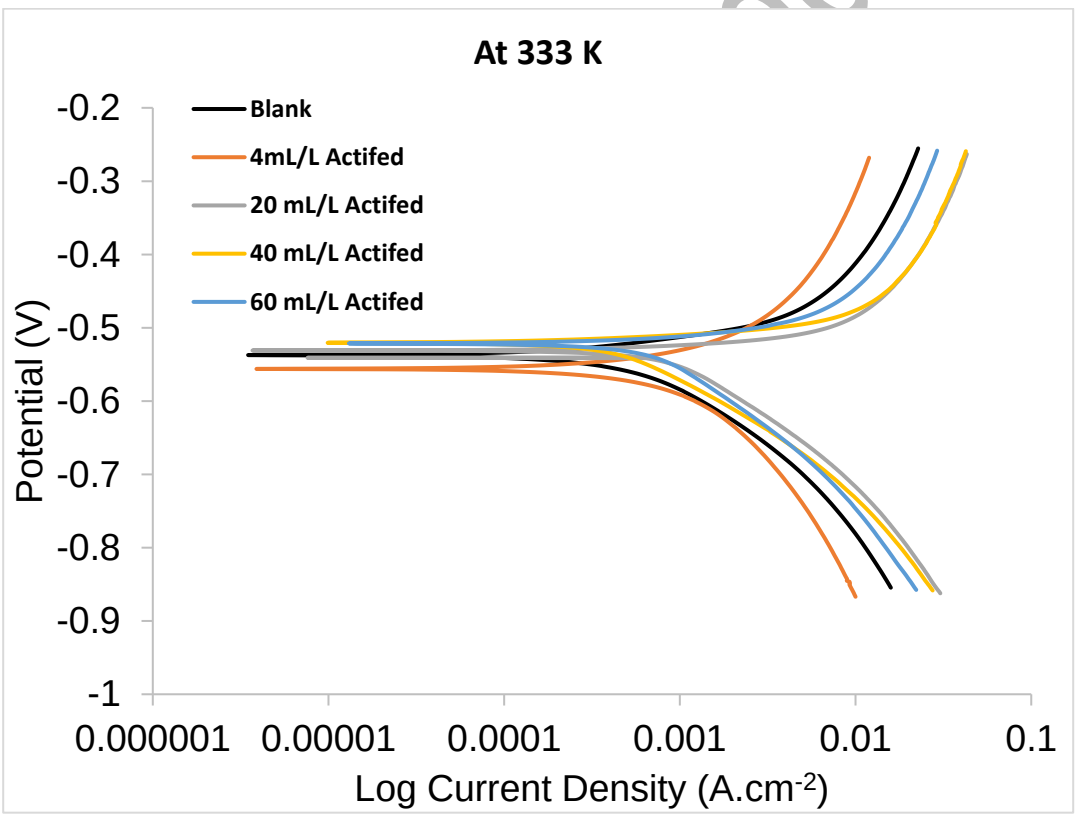

Fig. 2 Tafel plot for low-carbon steel in 0.5M H_3PO_4 at different ACD concentrations and temperatures.

Table 1 Electrochemical parameter of polarization diagrams for low-carbon steel in 0.5M H_3PO_4 at different ACD concentrations and temperatures.

Conc. Of Actifed	Temp. (K)	$-E_{corr}$ (V)	i_{corr} ($mA.cm^{-2}$)	$-b_c$ ($mV.dec^{-1}$)	$+b_a$ ($mV.dec^{-1}$)	IE (%)
Blank	303	0.539	0.57	155.21	42.94	---
	313	0.536	0.62	159.89	61.88	---
	323	0.538	0.72	165.39	67.26	---
	333	0.537	0.74	160.46	60.01	---
4 mL/L	303	0.549	0.388	46.40	37.53	31.9
	313	0.553	0.455	28.91	31.03	26.6
	323	0.550	0.4878	60.89	43.40	32.3
	333	0.556	0.641	52.17	43.32	13.4
20 mL/L	303	0.529	0.344	43.49	33.74	39.6
	313	0.531	0.387	43.43	27.85	37.6
	323	0.529	0.4351	86.15	21.66	39.6
	333	0.531	0.5287	57.88	16.28	28.6
40 mL/L	303	0.521	0.31	98.74	50.54	45.6
	313	0.522	0.35	56.26	21.23	43.5
	323	0.518	0.401	99.29	25.88	44.3
	333	0.520	0.417	87.58	22.92	43.6
60 mL/L	303	0.524	0.151	48.84	33.61	73.5
	313	0.517	0.175	42.81	24.02	71.8
	323	0.517	0.243	65.11	26.45	66.3
	333	0.521	0.284	85.14	19.33	61.6

3.2 SEM studies

Inhibited surfaces can be effectively characterized using scanning electron microscopy (SEM), which provides detailed insights into surface distinctions. Figure 3(a–c) illustrates these surface characteristics. The SEM image of the polished surface (Figure 3a) reveals a flat, smooth texture with minimal scratches caused by polishing, along with some signs of atmospheric corrosion likely resulting from sample storage. In contrast, the corroded surface (Figure 3b) exhibits uniform corrosion, characterized by the distribution of cathodic and anodic sites across the surface. For the inhibited surface (Figure 3), the SEM images highlight the adsorption process of ACD onto the metallic surface. The observed cracks are attributed to the drying of the protective film after it was removed from the electrolyte. These cracks are linked to the hydrophobic ends of the protective layer, which prevent moisture absorption. Studies have reported similar phenomena on protective layers formed by Methoprim [52] and urea-zinc sulfate-L-phenylalanine [53].

(a)

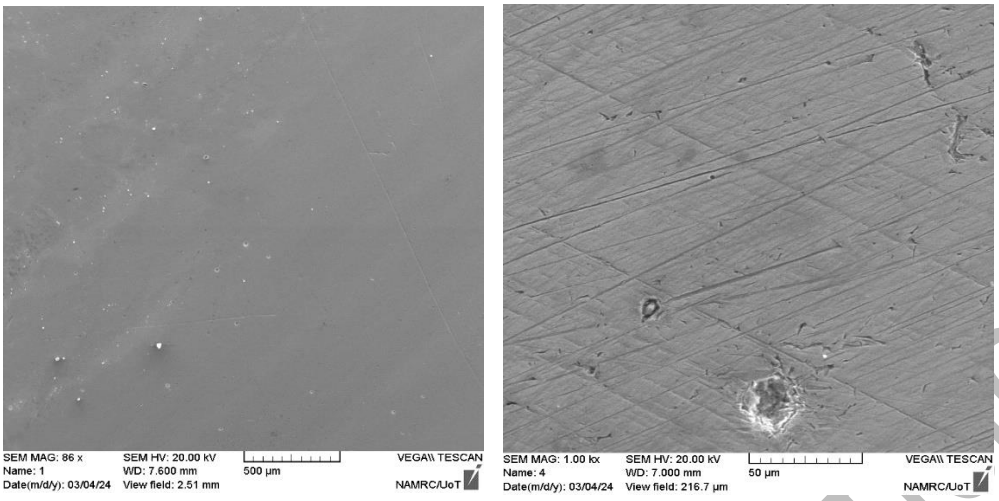

(b)

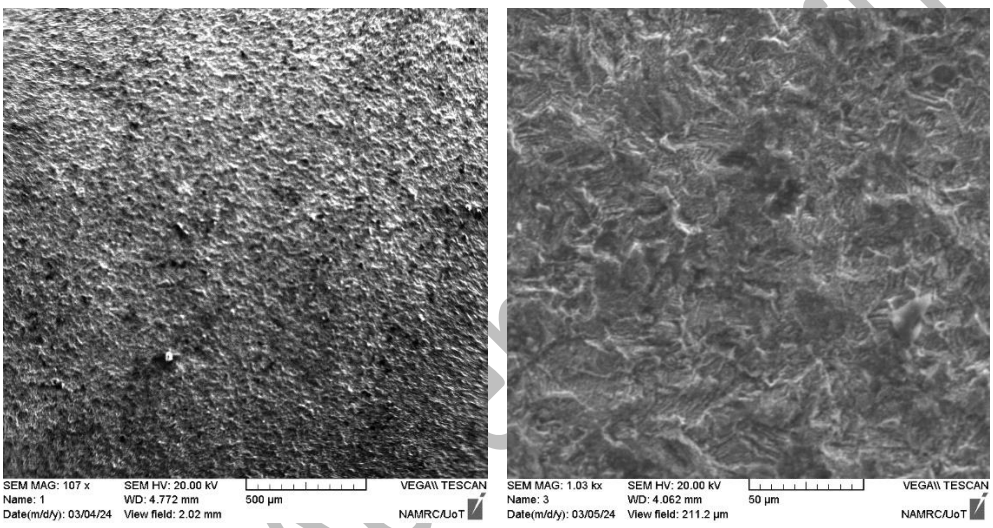

(c)

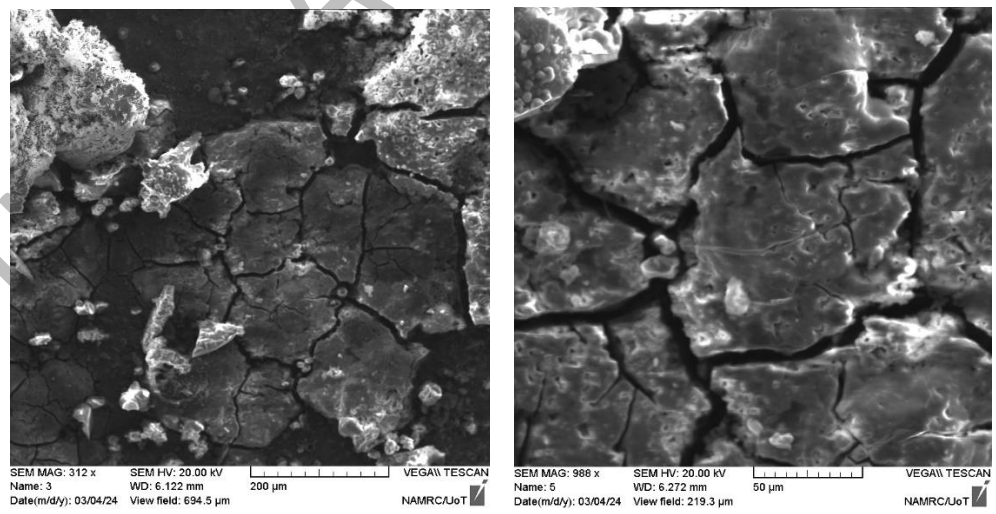

Fig. 3 SEM images of low-carbon steel in 0.5M H_3PO_4 with different ACD concentrations at 303 K. (a) Polished surface, (b) Corroded surface, (c) Protected surface.

3.3 FTIR studies

Actifed drug contains two components in its dose: phenylephrine and chlorpheniramine. Phenylephrine appears to have peaks corresponding to O–H stretching at 3266 cm^{-1}, C–H stretching at 2950 cm^{-1}, phenol at 1413 cm^{-1}, and C–N stretching at 1230 cm^{-1}. While for chlorpheniramine, it can be seen C–H stretching, C=N stretching at 1641 cm^{-1}, C=C stretching at ≈1600 $cm^{-1,}$ and C–H bending at 924 cm^{-1} (Fig. 4). FTIR for the film formed on the carbon steel surface after inhibition by expired Actifed within experimental conditions illustrates the groups that are attracted to the charged surface as a barrier for reducing corrosion. It was shown that the decrease in intensity took place in the stretching vibration for (O-H), which appeared in the range of 3400 – 2400 cm^{-1} as a broad band, as well as in the stretching vibration of (N-H, which appeared as a short peak in the range of 3500 – 3300 cm^{-1}. Finally, the decrease occurred in the stretching vibration for (C=C) in two peaks at 1600 and 1475 cm^{-1}. This means that these groups were incorporated in the adsorption process, and the decrease in intensities is attributed to the formation of complexes between these groups and ferrous ions rather than their being presented as free in solution, as suggested in Fig. 5.

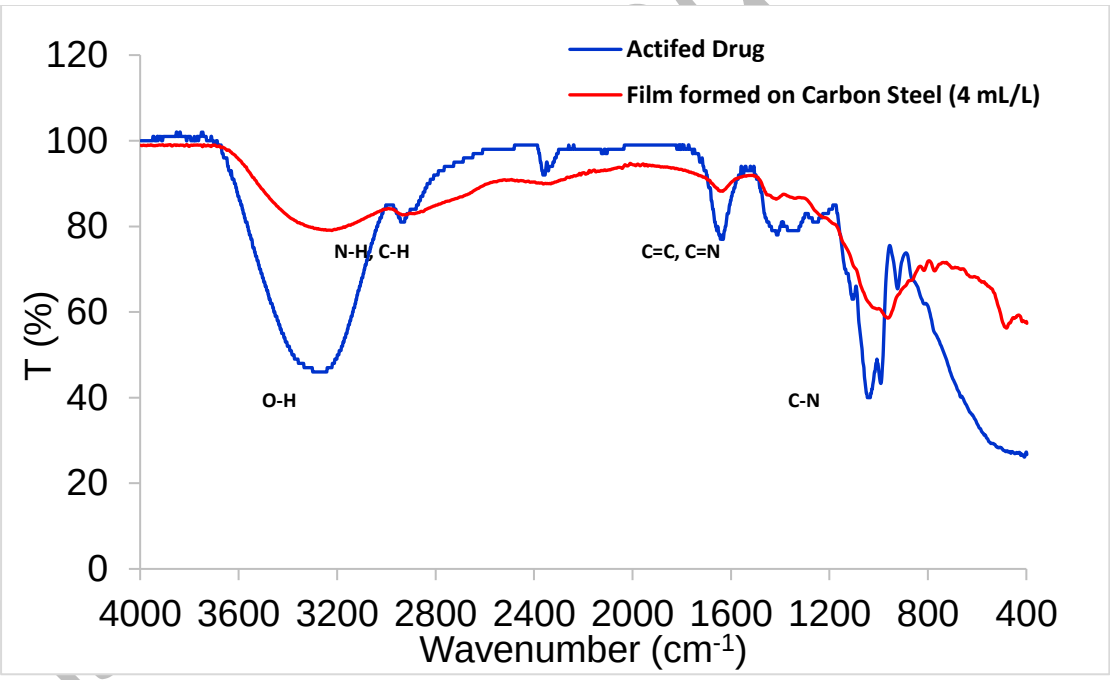

Fig. 4 FTIR of Actifed drug as it is and film formed by adsorption on the metal surface.

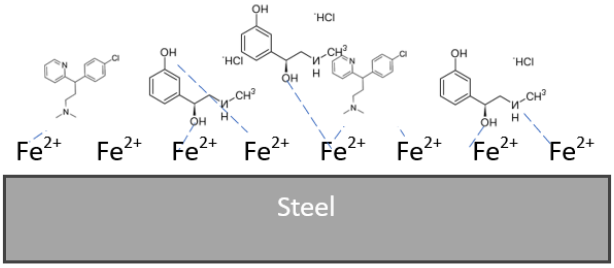

Fig. 5 Schematic mechanism of Iron (II)-Actifed coordinated complex.

3.4 Adsorption isotherms considerations

The adsorption isotherm determines how inhibitor chemicals interact with metal surfaces. Langmuir, Frumkin, Temkin, and Freundlich adsorption isotherms were tested. Extensive investigation has shown that the best model to fit electrochemical polarization data is the Freundlich adsorption isotherm (Eq. 4) [54]:

$$\theta = K_{ads} C^n \quad (4)$$

In Eq. 4, C represents the concentration of the inhibitor, θ signifies the fraction of the surface coverage, and K_{ads} denotes the equilibrium constant. Eq. 5 is illustrated in Fig. 6; the average correlation coefficient (R2) equals 0.966. Values of K_{ads} can be calculated from the intercept of Eq. 5. The average value of K_{ads} was 4671 l/ml. The typical adsorption-free energy (ΔG_{ads}) of ACD on low-carbon steel surfaces can be computed using Eq. 5.

$$\Delta G_{ads} = -RT \ln(55.5 K_{ads}) \quad (5)$$

The average value of ΔG_{ads} was -36.63 kJ/mol. The negative ΔG_{ads} value indicated the spontaneity of the adsorption process. Typically, ΔG_{ads} values approaching or slightly fewer negative than -20 kJ/mol often signify electrostatic interactions of charged molecules with the metal, suggesting physical adsorption. In contrast, values exceeding -40 kJ/mol signify chemisorption, suggesting a substantial charge transfer between molecules of organic material and a metal surface. Given that the average value of ΔG_{ads} lies between -20 and -40 kJ/mol, the adsorption process can be classified as mixed-mode adsorption, involving both physical and chemical mechanisms.

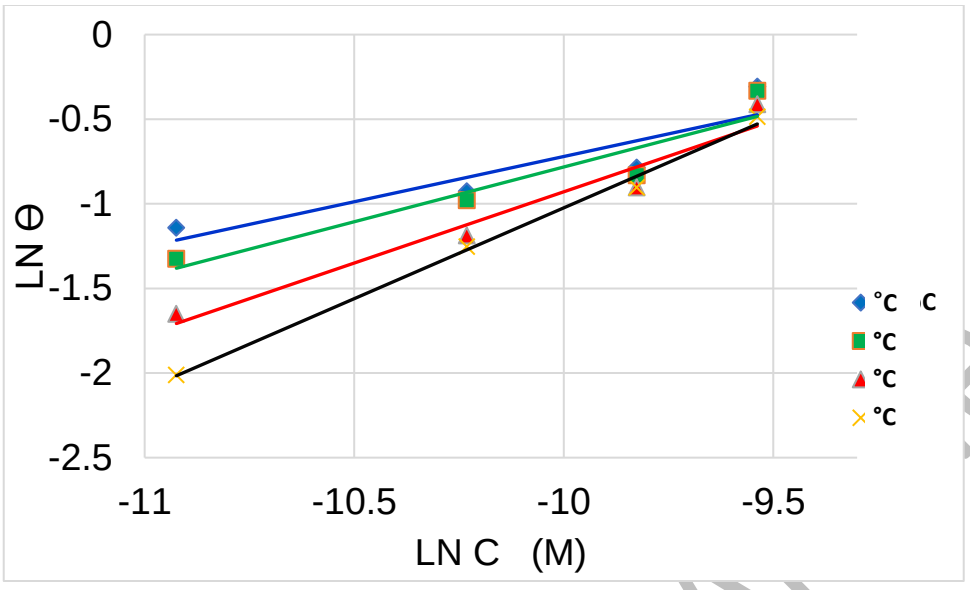

Fig. 6 Freundlich adsorption isotherm of ACD on low-carbon steel surface in 0.5M H_3PO_4 at different temperatures.

3.5 Kinetics considerations

The mechanism of corrosion inhibition by adsorption can be estimated by calculating the activation energies (E_a) during the process of corrosion in the presence and absence of Actifed by applying the linear form of Arrhenius equation (Eq. 6).

$$\ln i_{corr} = \ln A - \left[\frac{E_a}{RT}\right] \qquad 6$$

where A represents the frequency factor, T and R denote the absolute temperature and the gas constant, respectively. Plotting of ($\ln i_{corr}$) in the presence and absence of Actifed drug versus (1/T) in the range of experimental temperature (Fig. 7), yield a straight line with a slope ($\frac{-E_a}{R}$) as shown in Fig. 7. In the absence of ACD, the value of E_a was 7.85 kJ/mol, while in the presence of ACD, the values were 20.02, 16.9, 11.61, and 29.42 kJ/mol at 4, 20, 40, and 60 ml/l, respectively. The obtained results reveal that the presence of ACD leads to higher activation energy, which most likely means that the inhibitory effect produces a thin layer of resistance to the corrosion reaction of low-carbon steel in solution [55]. This increase in E_a is probably attributable to the establishment of electrostatic attractions between the metal surface and the inhibiting molecules in the solution. The higher E_a suggests that the protective layer created by ACD acts as a barrier, which slows down the corrosion process and enhances the material's resistance to corrosion.

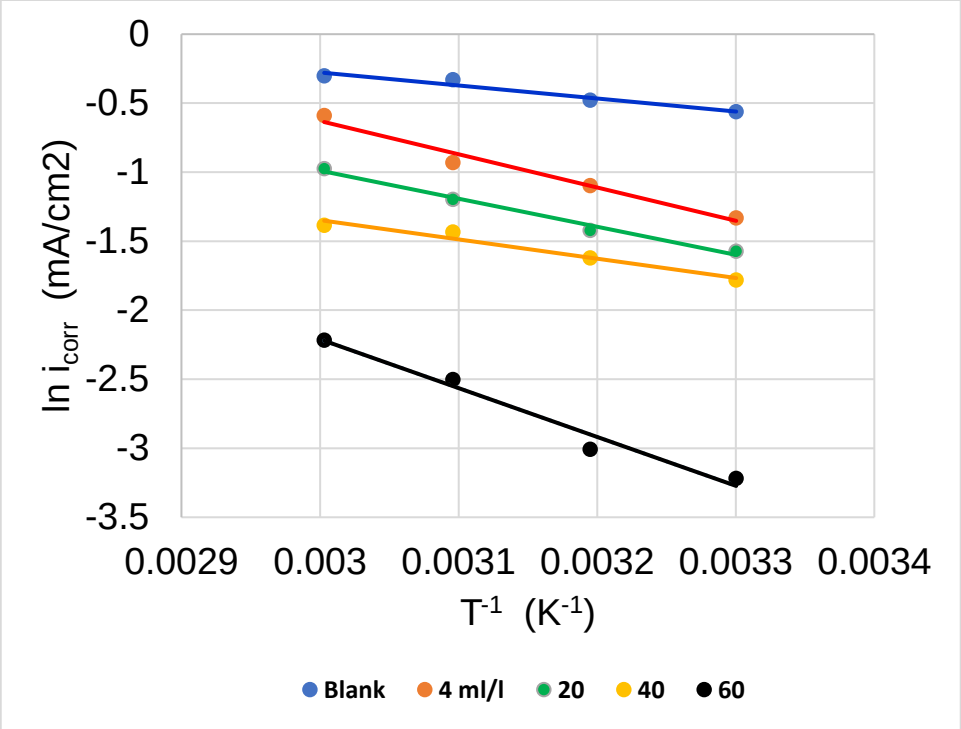

Fig. 7 Arrhenius plot of low-carbon steel in 0.5M H_3PO_4 at different concentrations of ACD and temperatures.

3.6 Quantum chemical considerations

The optimized structures, highest occupied molecular orbital (HOMO), lowest unoccupied molecular orbital (LUMO), and mapped-density structures of *pseudoephedrine hydrochloride* and *triprolidine hydrochloride*, which represent the main compounds of ACD syrup, were analyzed. The calculations were conducted in gaseous phases using density function theory (DFT). The ArgusLab software was utilized for the calculations, where geometry and energy optimizations were performed using the Austin Model 1 (AM1), with a limit of 200 iterations and a convergence threshold of 10^{-10} kcal/mol. A variety of quantum chemical parameters, including HOMO energy (E_{HOMO}), LUMO energy (E_{LUMO}), energy gap (ΔE), dipole moment (μ) and fraction of electron transferred (ΔN), were evaluated and presented in Table 2.

Donor-acceptor interactions are critical in understanding how inhibitor compounds adsorb onto metal surfaces. Based on frontier molecular orbital theory, the E_{LUMO} value indicates the inhibitor molecule's ability to receive electrons. On the other hand, E_{HOMO} is known for its ability to donate electrons. An inhibitor with an elevated E_{HOMO} value is more likely to give electrons to the metal's proper d-orbital. Conversely, a reduced E_{LUMO} value of the inhibitor suggests a greater likelihood of the molecule accepting electrons from the metal orbital during the back-donation [56-58]. The energy difference (ΔE) between E_{HOMO} and E_{LUMO} indicates the effectiveness of inhibitor molecules in terms of inhibition. The smaller the energy difference, the higher the inhibition value, as it implies less energy is required to extract electrons from the highest occupied molecular orbital.

ΔN is a critical quantity that quantifies the electron transfer between an inhibitory molecule and iron in a coordination reaction. It was calculated according to Eq. 7 [59]

$$\Delta N = \frac{X_{Fe} - X_{inh}}{2(\eta_{Fe} + \eta_{inh})} \quad (7)$$

$$\eta = \frac{E_{LUMO} - E_{HOMO}}{2} \quad (8)$$

$$\chi = -\mu = \frac{E_{LUMO} + E_{HOMO}}{2} \quad (9)$$

X_{Fe} and X_{inh} represent the absolute electronegativity of iron and the inhibitor molecule, respectively, while η_{Fe} and η_{inh} represent the iron's and the inhibitor molecule's absolute hardness, respectively. Equations 8 and 9 were used to determine the values of X and η for inhibitors. On the Pearson scale, X_{Fe} has a theoretical electronegativity value of 7, whereas η_{Fe} has a theoretical value of 0 eV/mol [60]. A high ΔN value (Table 2) indicates that the inhibitory molecule is responsible for providing electrons to iron, thereby enhancing the interaction between the metal and the ligand. This enhanced interaction not only boosts the stability of the complex but also increases the effectiveness of corrosion inhibition, reducing the reactivity of iron in a corrosive environment. Furthermore, the dipole moment is a crucial electronic parameter in corrosion studies, as it helps evaluate the strength of intermolecular interactions. This moment arises from the uneven distribution of electrical charges among the atoms within a molecule. Some researchers have suggested that an increase in the dipole moment correlates with enhanced inhibition efficacy [61]. Conversely, other studies have reported the association between dipole moment and inhibition efficiency is in inconsistent [62].

Table 2 Quantum chemical parameters of ACD.

Compound	**E_{HOMO} (eV)**	**E_{LUMO} (eV)**	**ΔE (eV)**	**μ (dybe)**	**ΔN**
Seudoephedrine	-9.471	0.187	9.283	2.279	0.244
Triprolidine	-6.663	-0.731	5.932	2.593	0.557

3.7 Antibacterial considerations

The observation of microbial activity was estimated to inhibit bacterial growth in experimental conditions due to the wide range of carbon steel tanks and pipes attached to soil or other bacteria-containing mediums. The inhibition zone of antibacterial activity of the Actifed drug was determined by the disk diffusion method using *Staphylococcus aureus* (gram-negative bacteria) and *E. coil* (gram-positive bacteria). Fig. 9 shows the inhibition zone that formed with a diameter of 19 mm for *Staphylococcus* and 13 mm for *E. coil*. This means using Actifed drug is an excellent option to prevent microbiological corrosion.

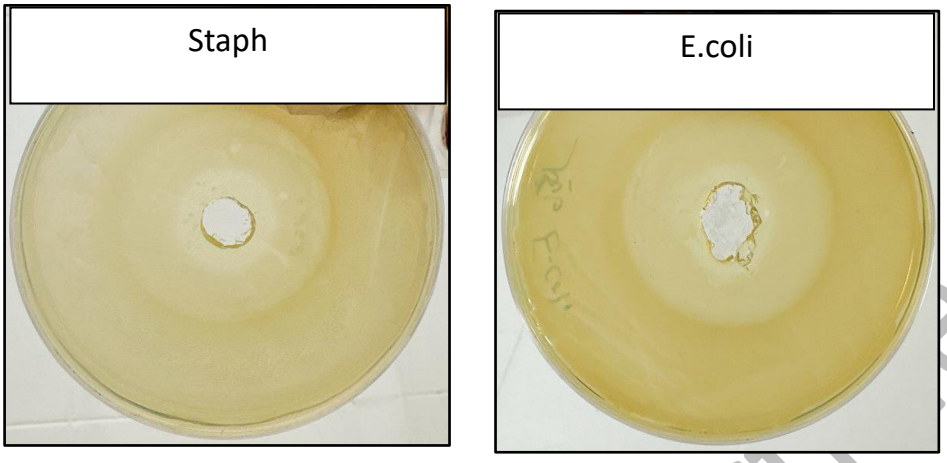

Fig. 9 The inhibition zone against two types of bacteria by Actifed drug.

4. Conclusion

The current study investigated an expired Actifed drug (ACD) as a corrosion inhibitor for protecting low-carbon steel in 0.5M H_3PO_4. The study used experimental and theoretical methodologies to evaluate the corrosion inhibiting efficacy of ACD. PDP, FTIR, SEM, and microbiological tests were used in the experimental process, while quantum chemical calculations were used in the theoretical analysis to clarify the interaction processes between the ACD and the low-carbon steel surface. The study found that ACD considerably decreases corrosion rates in acidic solutions, with an inhibitory efficiency of 73.5% at a concentration of 60 ml/l and 303 K. ACD was found to adsorb spontaneously on the metal surface, aligning with the Freundlich adsorption isotherm. FTIR, SEM, and theoretical examinations confirmed the electrochemical findings.

Statements and Declarations

Competing Interests: The authors declare no financial or commercial competing interests.

References

1- Wang, P. , Song, Y. , Fan, L. , Li, Z. , Ansari, K. R. , Talha, M. , Ansari, K. R. , Talha, M. , Singh, A. , and Lin, Y. (2024). Anticorrosion Evaluation of Novel Schiff-Imidazole Molecules for Q235 Steel in 1.0 mol/L HCl by Computational and Experimental Methodologies. *Journal of Molecular Structure*, 1306, 137793.

2- Jasim, Z. I. , Rashid, K. H. , AL-Azawi, K. F. , and Khadom, A. A. (2024). Optimization of the corrosion inhibition performance of novel oxadiazole thione-based Schiff base for mild steel in HCl media using Doehlert experimental design. *Inorganic Chemistry Communications*, 160, 111911.

3- Jasim, Z. I. , Rashid, K. H. , AL-Azawi, K. F. , and Khadom, A. A. (2023). Synthesis of schiff-based derivative as a novel corrosion inhibitor for mild steel in 1 M HCl solution: optimization, experimental, and theoretical investigations. *Journal of Bio-and Tribo-Corrosion*, *9* (3), 54.

4- Olajire, A. A. (2018). Recent advances on organic coating system technologies for corrosion protection of offshore metallic structures. *Journal of Molecular Liquids*, *269*, 572-606.

5- Bu, Y. , and Ao, J. P. (2017). A review on photoelectrochemical cathodic protection semiconductor thin films for metals. *Green Energy & Environment*, *2* (4), 331-362.

6- Li, J. , Kong, Z. , Liu, X. , Zheng, B. , Fan, Q. H. , Garratt, E. , Schuelke, T. , Wang, K. , Xu, H. , and Jin, H. (2021). Strategies to anode protection in lithium metal battery: A review. *InfoMat*, *3*(12), 1333-1363.

7- Khadom, A. A. (2015). Kinetics and synergistic effect of iodide ion and naphthylamine for the inhibition of corrosion reaction of mild steel in hydrochloric acid. *Reaction Kinetics, Mechanisms and Catalysis*, *115*, 463-481.

8- Ahmadi, S. , and Khormali, A. (2024). Optimization of the corrosion inhibition performance of 2-mercaptobenzothiazole for carbon steel in HCl media using response surface methodology. *Fuel*, *357*, 129783.

9- Jafari, H. , Akbarzade, K. , and Danaee, I. (2019). Corrosion inhibition of carbon steel immersedin a 1M HCl solution using benzothiazole derivatives. *Arabian Journal of Chemistry*, *12*, 1387–1394, http://dx.doi.org/10.1016/j.arabjc.2014.11.018

10- Jafari, H. , Ameri, E. , Rezaeivala, M. , Berisha A. , and Halili, J. (2022). Anti-corrosion behavior of two N2O4 Schiff-base ligands: Experimental and theoretical studies Author links open overlay panel. *Journal of Physics and Chemistry of Solids*, 164 (7), 110645, https://doi.org/10.1016/j.jpcs.2022.110645

11- Jafari, H. , Danaee, I. , Eskandari, H. , and Avei, M. R. (2014). Combined Computational and Experimental Study on the Adsorption and Inhibition Effects of N2O2 Schiff Base on the Corrosion of API 5L Grade B Steel in 1 mol/L HCl. *Journal of Materials Science & Technology*, 30 (3), 239-252, https://doi.org/10.1016/j.jmst.2014.01.003

12- Jafari, H. , Ameri, E. , Rezaeivala, M. , and Berisha, A. (2022). Experimental and theoretical studies on protecting steel against 0.5 M H2SO4 corrosion by new schiff base. *Journal of the Indian Chemical Society*, 99 (9), 100665, https://doi.org/10.1016/j.jics.2022.100665

13- Mohsenifar, F., Jafari, H. , and Sayin, K. (2016). Investigation of Thermodynamic Parameters for Steel Corrosion in Acidic Solution in the Presence of N,N′-Bis(phloroacetophenone)-1,2 propanediamine. *Journal of Bio- and Tribo-Corrosion*, 2, 1.

14- Jafari, H., Ameri, E., Rezaeivala, M., Berisha, A. , and Vakili, M. H. (2022). Comparison the anticorrosion behavior of three symmetrical Schiff-base ligands: experimental and theoretical studies. *Journal of Applied Electrochemistry*, 52, (7), 10.1007/s10800-022-01748-0

15- Jafari, H. , and Sayin, K. (2016). Sulfur containing compounds as corrosion inhibitors for mild steel in hydrochloric acid solution. *Transactions of the Indian Institute of Metals*, 69, 805–815,

16- Jafari, H. , Rezaeivala, M. , Mokhtarian, N. , Berisha, A. , and Ameri E. (2022). Corrosion Inhibition of Carbon Steel in 0.5 M H2SO4 by New Reduced Schiff Base Ligand. *Journal of Bio- and Tribo-Corrosion*, 8:81, https://doi.org/10.1007/s40735-022-00679-9

17- Al-azawi, K. F. , Ahmed, Z. W. , Ali, E. H. , Khadom, A. A. , Abrahim, H. H. , Rashid, K. H. (2023). Synthesis and characterization of (E)-4-(((4-(5-mercapto-1, 3, 4-oxadiazol-2-yl) phenyl) amino) methyl)-2-methoxyphenol as a novel corrosion inhibitor for mild-steel in acidic medium. *Results Chem. ,* **5**, 100975.

18- Dehghani, A. , Ghahremani, P. , Mostafatabar, A. H. , and Ramezanzadeh, B. (2024). Plant extracts: Probable alternatives for traditional inhibitors for controlling alloys corrosion against acidic media—A review. *Biomass Conversion and Biorefinery*, *14*(6), 7467-7486.

19- Eddy, N. O. , Stoyanov, S. R. , and Ebenso, E. E. (2010). Fluoroquinolones as corrosion inhibitors for mild steel in acidic medium; experimental and theoretical studies. *International Journal of Electrochemical Science*, *5*(8), 1127-1150.

20- Eddy, N. O. , and Ebenso, E. E. (2010). Corrosion inhibition and adsorption characteristics of Tarivid on mild steel in H2SO4. *Journal of Chemistry*, *7*, S442-S448.

21- Hameed, R. A. (2011). Ranitidine drugs as non-toxic corrosion inhibitors for mild steel in hydrochloric acid medium. *Port Electrochim Acta*, *29*(4), 273-285.

22- Naqvi, I. , Saleemi, A. R. , and Naveed, S. (2011). Cefixime: A drug as Efficient Corrosion Inhibitor for Mild Steel in Acidic Media. Electrochemical and Thermodynamic Studies. *International journal of electrochemical science*, *6*(1), 146-161.

23- Abdallah, M. , Zaafarany, I. , Al-Karanee, S. O. , and Abd El-Fattah, A. A. (2012). Antihypertensive drugs as an inhibitors for corrosion of aluminum and aluminum silicon alloys in aqueous solutions. *Arabian Journal of Chemistry*, *5*(2), 225-234.

24- Fouda, A. S. , Elmorsi, M. A. , Fayed, T. A. , Hassan, A. F. , and Soltan, M. (2014). Corrosion inhibitors based on antibiotic derivatives for protection of carbon steel corrosion in hydrochloric acid solutions. *International Journal of Advanced Research*, *2*(4), 788-807.

25- Mahdi, A. S. (2014). Amoxicillin as green corrosion inhibitor for concrete reinforced steel in simulated concrete pore solution containing chloride. *International Journal of Advanced Research in Engineering and Technology*, *5*, 99-107.

26- Akpan, I. A. , and Offiong, N. O. (2014). A modiaquine drug as a corrosion inhibitor for mild steel in 0.1 M HCl solution. *Chemistry of metals and alloys*, 7, 149-153.

27- Attia, E. M. (2015). Expired Farcolin drugs as corrosion inhibitor for carbon steel in 1 M HCl solution. *Journal of Basic and Applied Chemistry*, *5*(1), 1-15.

28- Singh, P. , Chauhan, D. S. , Srivastava, K. , Srivastava, V. , and Quraishi, M. A. (2017). Expired Atorvastatin drug as corrosion inhibitor for mild steel in hydrochloric acid solution. *International Journal of Industrial Chemistry,* 8, 363-372.

29- Verma, D. , and Khan, F. (2016). Corrosion inhibition of mild steel by using Sulpha drugs in phosphoric acid medium: A combined experimental and theoretical approach. *American Chemical Science Journal*, *14*(3), 1–8. https://doi.org/10.9734/acsj/2016/26282

30- Ikpi, M. E. , Abeng, F. E. , and Okonkwo, B. O. (2017). Experimental and computational study of Levofloxacin as corrosion inhibitor for carbon steel in acidic media. *World News of Natural Sciences*, 9, 79-90.

31- Anaee, R. A. , Tomi, I. H. R. , Abdulmajeed, M. H. , Naser, S. A. , and Kathem, M. M. (2019). Expired Etoricoxib as a corrosion inhibitor for steel in acidic solution. *Journal of Molecular Liquids*, *279*, 594-602.

32- Anaee, R. A. , Abd Al-Majeed, M. H. , Naser, S. A. , Kathem, M. M. , and Ahmed, O. A. (2019). Antibacterial inhibitor as an expired Metoclopramide in 0.5 M phosphoric acid. *Al-Khwarizmi Engineering Journal*, 15 (1), 71-81.

33- Alkarim, T. A. , Al Azawi, K. F. , and Anaee, R. A. (2021). Green approach to corrosion inhibition of aluminum in acidic solutions by the expired drug and biological activity. *Biochemical and Cellular Archives*, 21 (2), 3557-3569.

34- Alkarim, T. A. , Al Azawi, K. F. , and Anaee, R. A. (2021). Anticorrosive properties of Spiramycin for aluminum in acidic medium. *International Journal of Corrosion and Scale Inhibition*, 10 (3), 1168-1188.

35- Alkarim, T. A. , Al Azawi, K. F. , and Anaee, R. A. (2023). Experimental Study and Quantum Calculations for Spiramycin and Isosorbide Dinitrate as Corrosion Inhibitors. *Journal of Applied Sciences and Nanotechnology*, 3 (1), 18-33.

36- Abdullah, H. A. , Anaee, R. A. , and Khadom, A. A. (2022). Expired Metheprim drug as a corrosion inhibitor for aluminum in 1 M HCl solution: Experimental and theoretical studies. *Int. J. Corros. Scale Inhib*, 11 (3), 1355-1373.

37- Al-Ghaban, A. M. , Abdullah, H. A. , Anaee, R. A. , Naser, S. A. , and Khadom, A. A. (2023). Expired Butamirate drug as eco-friendly corrosion inhibitor for aluminum in seawater: Experimental and theoretical studies. *Journal of Engineering Research,* 12 (3), 299-309.

38- Maged, S. A. , Anaee, R. A. , and Mathew, M.T. (2023). Negative effect of calcium tablets on the corrosion of a Co–Cr–Mo alloy as an implant, *Int. J. Corros. Scale Inhib*. , 12 (1), 275-291.

39- Maged, S. A. , Anaee, R. A. , and Mathew, M.T. (2023). The Role of Uric Acid to Reduce the Corrosion of Co-Cr-Mo Alloy as Joint in Presence of Ca and Vitamin D3. *Journal of Bio- and Tribo-Corrosion*, 9:66. https://doi.org/10.1007/s40735-023-00786-1

40-Hatem, S. Ammar , Alsultanilani, K. F. and Ajjam, S. Kathim (2024). Effect of Ultrasound on the Performance of Salicornia Extract as an Eco-Friendly Corrosion Inhibitor. *Iranian Journal of Chemistry and Chemical Engineering*, *43*(4), 1685-1695. doi: 10.30492/ijcce.2023.2004573.6073

41- Mulky, L. and Rao, P. (2023). Exploring the Potential of a Plant Extract in Mitigating Corrosion under Jet Impingement Conditions. *Iranian Journal of Chemistry and Chemical Engineering*, *42*(11), 3887-3897. doi: 10.30492/ijcce.2023.1986359.5788

42-Jafari, N. , Ahmadi, S. A. and Razavi, R. (2023). Experimental and Computational Study of Trachyspermum Leaves Extract as a Green Inhibitor for Corrosion Inhibition of Mild Steel in HCl. *Iranian Journal of Chemistry and Chemical Engineering*, *42*(10), 3324-3337. doi: 10.30492/ijcce.2023.1971031.5659

43- Kherraf, S. , Khelfaoui, M. , Boughaita, I. , Marsa, Z. and Medjram, M. S. (2023). Lavandula Stoechas as a Green Corrosion Inhibitor for Monel 400 in Sulfuric Acid: Electrochemical, Gravimetrical, and AFM Investigations. *Iranian Journal of Chemistry and Chemical Engineering*, *42*(8), 2538-2549. doi: 10.30492/ijcce.2023.563710.5656

44- Khormali, A. and Ahmadi, S. (2023). Synergistic Effect Between Oleic Imidazoline and 2-Mercaptobenzimidazole for Increasing the Corrosion Inhibition Performance in Carbon Steel Samples. *Iranian Journal of Chemistry and Chemical Engineering*, *42*(1), 321-336. doi: 10.30492/ijcce.2022.546098.5091

45- Bhawsar, J. and Jain, P. (2022). Corrosion Inhibition Potential of Mentha spicata Extract on Mild Steel in Acidic Medium. *Iranian Journal of Chemistry and Chemical Engineering*, *41*(10), 3365-3376. doi: 10.30492/ijcce.2022.531824.4786

46- Shwethambika, P. and Ishwara Bhat, J. (2021). Matured Theobroma Cocoa Pod Extracts as Green Inhibitor for Acid Corrosion of Aluminium. *Iranian Journal of Chemistry and Chemical Engineering,* 40(3), 906-919. doi: 10.30492/ijcce.2020.38022

47- Aljaafari, H. A. S. , Ali, S. B. , Abbas, M. A. , Ali, H. B. , Anaee, R. A. , Naser, S. A. , Mahdi, R. I. , and Anaee, M. A. (2024). Improvement in the Corrosion Behavior of Al-Si-xWC Composites Prepared by Casting Technique. *Journal of Bio- and Tribo-Corrosion,* 10:100 https://doi.org/10.1007/s40735-024-00902-9

48- Abdulaah, H. A. , Al-Ghaban, A. M. , Anaee, R. A. , Khadom, A. A. , and Kadhim, M. M. (2023). Cerium-tricalcium phosphate coating for 316L stainless steel in simulated human fluid: Experimental, biological, theoretical, and electrochemical investigations. *Journal of Electrochemical Science and Engineering*, *13*(1), 115-126.

49- Anaee, R. A. (2014). Thermodynamic and Kinetic Study for Corrosion of Al-Si-Cu/Y2O3 Composites. *Asian Journal of Chemistry*, 26(14), 4469-4474, DOI:10.14233/ajchem.2014.17005.

50- Abdullah, H. A. , Anaee, R. A. , Khadom, A. A. , Abd-Ali, A. T. , Malik, A. H. , Kadhim, M. M. (2023). Experimental and theoretical assessments of the chamomile flower extract as a green corrosion inhibitor for aluminum in artificial seawater. *Results in Chemistry.* 6, 101035, https://doi.org/10.1016/j.rechem.2023.101035

51- Anaee, R. A. (2016). Behavior of Ti/HA in Saliva at different temperatures as restorative materials, *Journal of Bio- and Tribocorrosion*. 2 (5), 16-36, DOI 10.1007/s40735-016-0036-1.

52- Hafiz, M. H. , Anaee, R. A. , Noor, R. S. , and Wehib, M. A. (2013). phenylenediamine as inhibitor in sour water at oil refinery. *Int. J. Electrochem. Sci. ,* 8 (12), 12402-12416.

53- Manoharan, G., Nithyanandam R., Antony, J. S. , and Rajendran, S. (2025). Investigating the Effects of Urea-Zinc Sulfate-L Phenylalanine on the Corrosion Inhibition of Mild Steel Exposed to pH-4 Sulfuric Acid. *Current Analytical Chemistry*, 21 (1), 68-78, DOI: 10.2174/0115734110296231240501170801

54- Najm, N. , Ataiwi, A. H. and Anaee, R. A. (2022). Annealing and Coating Influence on the Mechanical Properties, Microstructure, and Corrosion Properties of Biodegradable Mg Alloy (AZ91). *Journal of Bio- and Tribo-Corrosion,* 8:64.

55- Jedy, H. M. , Anaee, R. A. , Abdulkarim, A. A. , and Mathew, T. M. (2021). The Effect of Nb2O5-Ni Coatings on the Microstructural and Corrosion Behavior on Carbon Steel for Marine Application. *Journal of Bio- and Tribo-Corrosion*, 7(1), https://doi.org/10.1007/s40735-020-00440-0

56- Jessam, R. A. , and Hamdi, S. S. (2024). Drag reduction in pipelines flow using passive flow control, *AIP Conf. Proc.* , 3002, 040003 https://doi.org/10.1063/5.0206518

57- Hamdi, S. S. , Al-Kayiem, H. H. , Muhsan, A. S. , Magari, E. (2020). Experimental dataset on the dispersion stability of natural polymer non-covalently functionalized graphene nanoplatelets in high salinity brines. *Data in Brief*, 31, 105702, https://doi.org/10.1016/j.dib.2020.105702

58- Ishtiaq, U. , Aref, A. , Muhsan, A. S. , Rashid, A. , Hamdi, S. S. (2022). High strength glass beads coated with CNT/rGO incorporated urethane coating for improved crush resistance for effective hydraulic fracturing. *Journal of Petroleum Exploration and Production Technology*, 12:2691-2697, https://doi.org/10.1007/s13202-022-01468-3

59- Kumar, H. , and Yadav, V. (2021). Highly efficient and eco-friendly acid corrosion inhibitor for mild steel: Experimental and theoretical study. *Journal of Molecular Liquids*, *335*, 116220.

60- Verma, C. , Saji, V. S. , Quraishi, M. A. , and Ebenso, E. E. (2020). Pyrazole derivatives as environmental benign acid corrosion inhibitors for mild steel: Experimental and computational studies. *Journal of Molecular Liquids*, *298*, 111943.

61- Rasul, H. H. , Mamad, D. M. , Azeez, Y. H. , Omer, R. A. , and Omer, K. A. (2023). Theoretical investigation on corrosion inhibition efficiency of some amino acid compounds, *Computational and Theoretical Chemistry*, *1225*, 114177.

62- Jawad, Q. A. , Hameed, A. Q. , Abood, M. K. , Al-Amiery, A. A. , Shaker, L. M. , Kadhum, A. A. H. , and Takriff, M. S. (2020). Synthesis and comparative study of novel triazole derived as corrosion inhibitor of mild steel in hcl medium complemented with the calculations. *International Journal of Corrosion and Scale Inhibition*, 9 (2), 688-705.